Effect of Seismic Action on Settlement and Load Sharing of Piled Rafts Based on Field Monitoring

K. Yamashita[1], J. Hamada[2] and T. Tanikawa[3]
[1,2,3]*Takenaka Research and Development Institute, Takenaka Corporation, Chiba, Japan*
E-mail: yamashita.kiyoshi@takenaka.co.jp

ABSTRACT: This paper offers three case histories of piled rafts combined with deep mixing wall grids, in which long-term monitoring on settlement and load sharing between the piles and the raft was performed. The buildings are located on soft ground consisting of liquefiable sand and soft clayey soil. The buildings experienced the 2011 Tohoku Earthquake (M=9.0, about 380 km distance from the epicentre) and the seismic response during the earthquake was successfully recorded for the two buildings. Based on the static and dynamic monitoring results, the effect of seismic action on the settlement and load sharing between the piles and the raft were investigated. It was found that no significant change in foundation settlement was observed after the earthquake. However, some change in load sharing between the piles and the raft caused by the seismic action was noted for the relatively short shaft-bearing piles, while almost no change in the load sharing was observed for the toe-bearing piles or long shaft-bearing piles.

KEYWORDS: Piled raft foundation, Deep mixing wall grid, Soft ground, Settlement, Load sharing, Field monitoring, The 2011 Tohoku Earthquake

1. INTRODUCTION

In recent years there has been an increasing recognition that combining a raft with piles to reduce raft settlement can lead to considerable economy without compromising the safety and performance of the foundation (Poulos, 2001). A piled foundation combining piles and raft response in a design is here called "piled raft". The effectiveness of piled rafts in reducing average and differential settlements has been confirmed not only on favorable ground conditions as shown by Katzenbach et al. (2000) and Mandolini et al. (2005), but also in case of unfavorable conditions with ground improvement techniques (Yamashita et al., 2011a, 2011b, 2012). Recently, it has become necessary to develop more reliable design methods for piled rafts as cost effective solutions, particularly in highly active seismic areas. Seismic action will induce additional lateral forces and the consequent moments in the structure and also induce lateral motions in the ground. Hence, the effects of inertial and kinematic forces on the foundation system should be considered (Poulos, 2016). However, case histories on static and seismic monitoring of full-scale piled rafts subjected to seismic loading are very limited (Mendoza et al., 2000; Hamada et al., 2015).

This paper offers three case histories of piled rafts combined with deep mixing wall grids in soft ground, in which long-term monitoring on settlement and load sharing between the piles and the raft was performed. After the end of the construction (denoted E.O.C., hereafter), the buildings experienced the 2011 Tohoku Earthquake and the seismic responses during the earthquake were successfully recorded for the 12-story and 7-story buildings. Based on the static and dynamic monitoring results, the effect of seismic action on the settlement and on the vertical load sharing between the piles and the raft were investigated.

2. CASE HISTORIES

The schematics of the three structures with the soil profiles are shown in Figure 1 and the foundation plans are illustrated in Figure 2. The 12-story residential building, 7-story office building and 4-story parking garage are located on soft ground consisting of liquefiable sand and thick soft clayey soil. Table 1 presents an overview of the structures and foundations. Both the 12-story building and the 7-story building are located in Toyo, Tokyo; the 7-story building about 700 m east of the 12-story building. The 4-story building is located in Urayasu City, about 7-km south-east of Toyo.

2.1 Soil conditions

The soil conditions at the 12-story and 7-story buildings are similar. The soil profile down to a depth of 7-10 m consists of fill, soft silt, and loose silty sand above an alluvial stratum of silty soil. To a depth of about 45 m, very-soft to medium alluvial silty soil exists that is slightly overconsolidated with an OCR of 1.1-1.5 above 16-18 m depth. The groundwater table appears 1.5-2.0 m below the ground surface. Below about 45-m depth, there is a Pleistocene dense sandy layer. Downhole shear wave velocities were 110 to 240 m/s to the depth of about 40 m, and those in the very dense sandy strata below a depth of about 50 m were 350 to 610 m/s.

Table 1 Case histories

Structure	Site	Construction period	Average stress (kPa)	Foundation depth (m)	Groundwater table (m)	Thickness of foundation slab (m)	Pile			
							Number	Toe depth (m)	Diameter (m)	Pile type
12-story building (residence)	Tokyo	2007-08	199	4.8	1.8	1.5	16	50	0.8-1.2	SC & PHC (pre-boring)
7-story building (office)	Tokyo	2003-04	100	1.6 & 2.2	1.5	0.3	70	30	0.6-0.9	PHC (pre-boring)
4-story building (parking garage)	Chiba	2006	45	1.2-2.4	1.5	0.45	152	35-42 (N) 62 (S)	0.5-1.0	PHC (pre-boring)

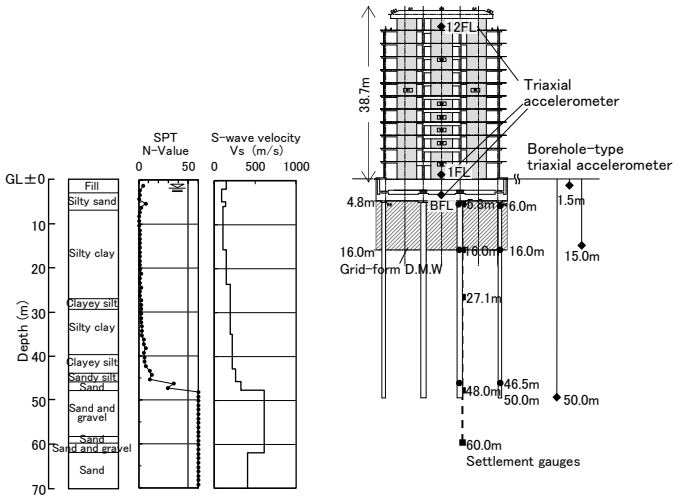

(a) 12-story building

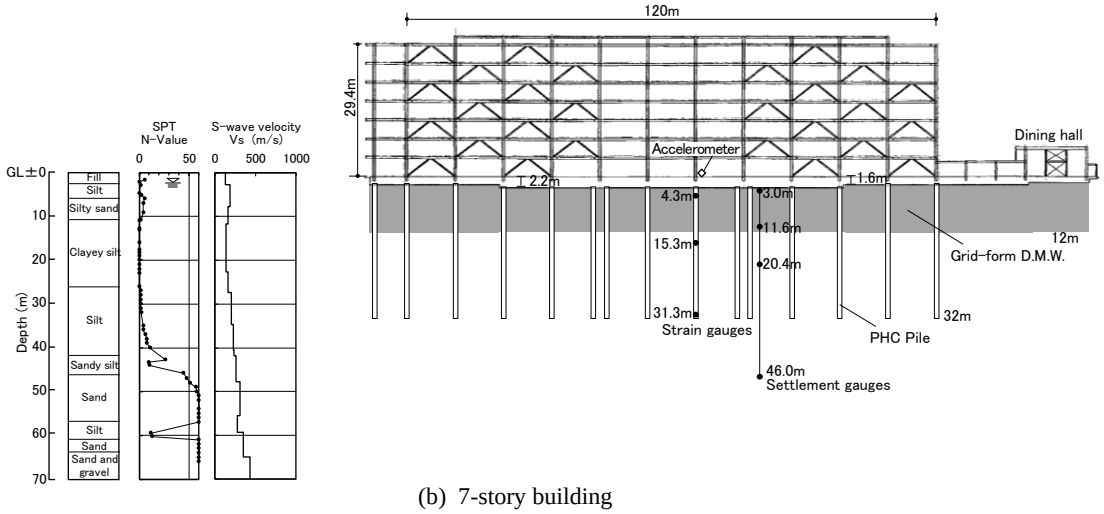

(b) 7-story building

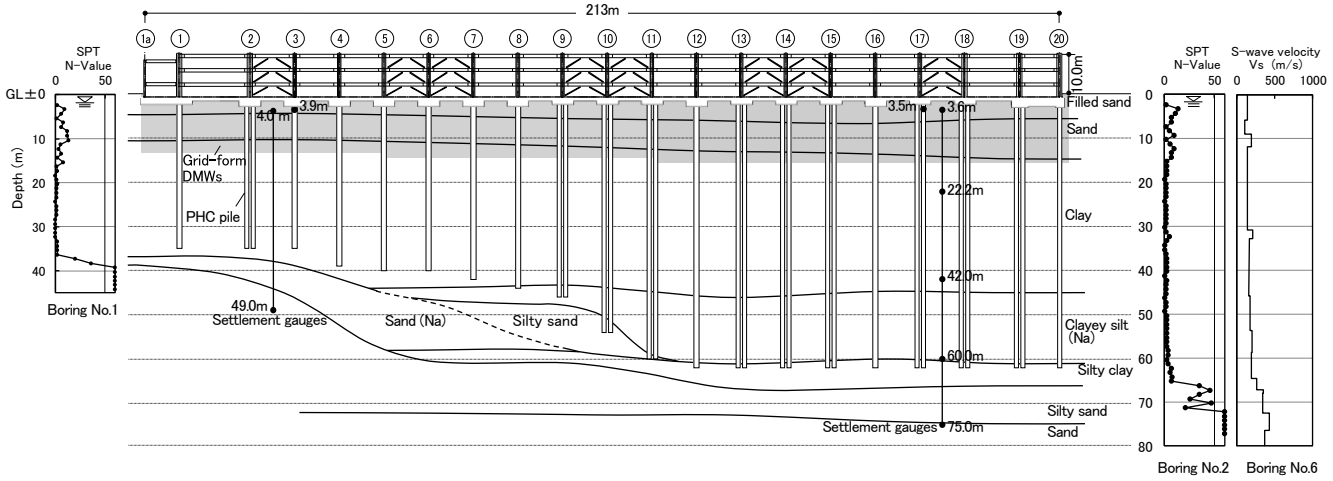

(c) 4-story building

Figure 1 Schematics of three structures with soil profiles

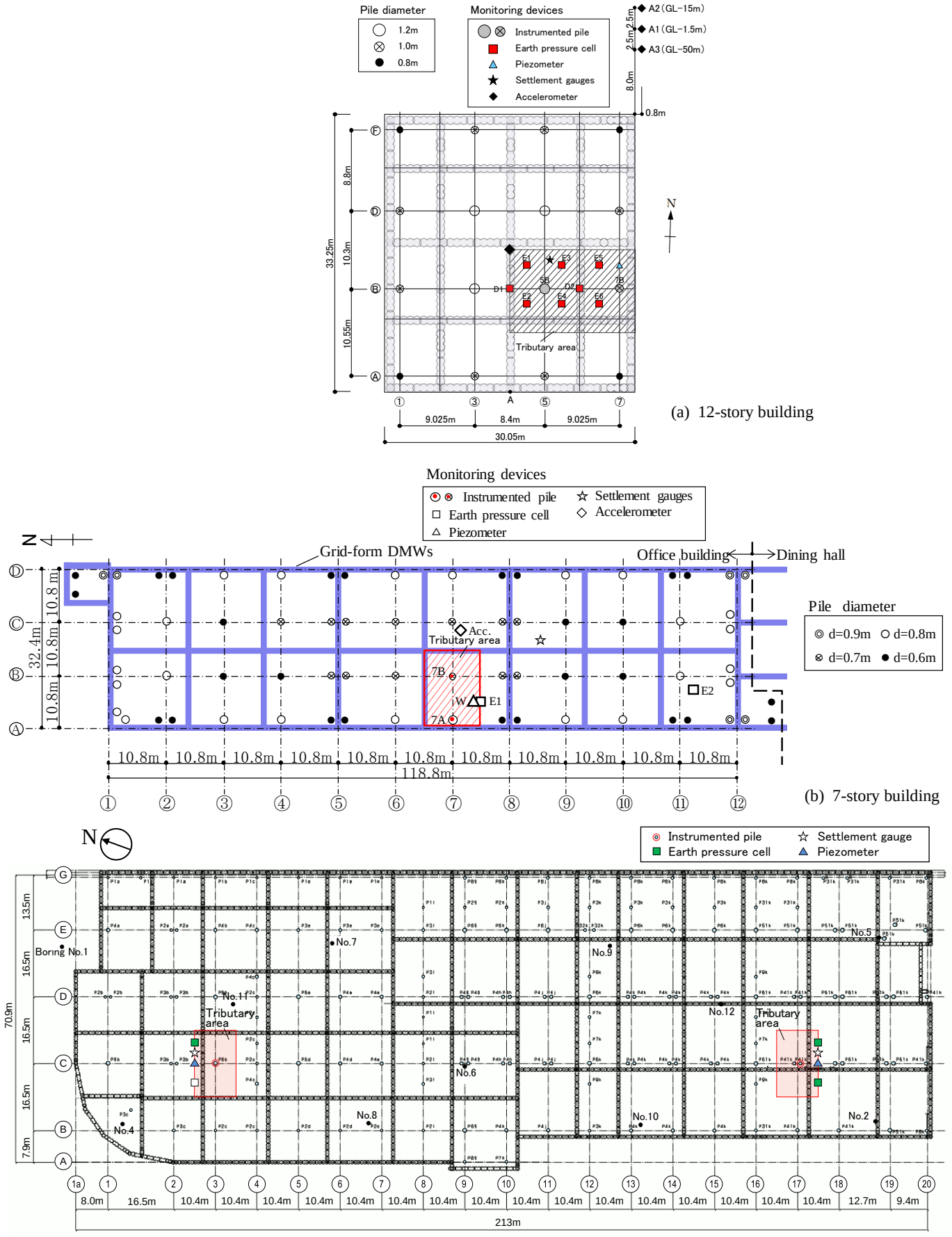

Figure 2 Foundation plan with locations of monitoring devices

The 4-story building in Urayasu City is located in a reclaimed land where the reclamation work was ended in 1975. The soil profile down to a depth of 10-15 m from the ground surface consists of filled sand and alluvial loose sand. The ground water table is about 1.5 m below the ground surface. Below the depth of 16 m, there are very-soft to medium alluvial clay layers which are normally consolidated or undergoing consolidation. The thickness of the alluvial clay layers changes markedly in the north-south direction near the center of the site since a buried valley exist below the site. Below about 60-m depth, the soil comprises a Pleistocene medium to stiff silty clay. Pleistocene dense sandy layers appear at a depth of about 39 m in the northern part and 66 m in the southern part.

2.2 Foundation design

The 12-story building is a reinforced concrete structure with a seismic base isolation system. The average stress, which corresponds to the sum of the dead load and the live load of the building in the structural design divided by its footprint, was 199 kPa. To reduce the average and differential settlement due to consolidation of the very soft clayey layers to an acceptable level, SC (steel pipe-concrete composite) and PHC (pretensioned spun high-strength concrete) piles, 45-m long and 0.8 to 1.2 m in diameter, were employed as settlement reducers. The pile toes reached the very dense sand-and-gravel sufficiently well enough to ensure the toe resistance. The piles were constructed by inserting a set of pile segments into a pre-augered borehole filled with mixed-in-place soil cement. Similar pile construction methods were used in the other two structures.

The 7-story building is a steel-frame structure. The average stress was 100 kPa. Shaft-bearing piles (28-m long PHC piles, 0.6 to 0.9 m in diameter) were employed to serve as settlement reducers.

The 4-story building is a steel reinforced concrete columns and steel beams. The average stress was 45 kPa. PHC piles, 0.5 to 1.0 m in diameter, were used as friction piles. The depths of the pile toe is 35-42 m from the ground surface in the northern part and 62 m in the southern part. In the design, resistance of the raft was considered in the northern part, while a conventional pile foundation was employed in the southern part because long-term resistance of the raft could not be relied on due to the residual subsidence.

As a countermeasure of liquefaction of the loose silty sand (12-story and 7-story buildings) or the loose sand (4-story building) underneath the raft due to strong ground motions, grid-form deep mixing walls (DMWs) were employed. The design standard compressive strength of the cement stabilized soil was 1.8 MPa. The area replacement ratio (area of the DMWs in plan divided by the total area) was approximately 0.25, 0.10 and 0.12 for the 12-story, 7-story and 4-story buildings, respectively. Note that, in the 12-story building, the grid-form DMWs were constructed to a depth of 16 m with the bottom being embedded in the stiff silty clay to improve the stiffness of the soil underneath the raft. The layout of the piles and the grid-form DMWs with the locations of the monitoring devices are shown in Figure 2. Accelerometers were installed at three depths below the ground surface near the 12-story building, in addition, accelerometers were installed on the 12-story and 7-story buildings as shown in Figures 1(a) and 1(b).

Further details in soil conditions, foundation design and instrumentation, as well as the monitoring results, were described in previous papers: Yamashita et al. (2012), (2017) for the 12-story building, Yamashita et al. (2016) for the 7-story building and Yamashita et al. (2019) for the 4-story building. In this paper, the effects of seismic action on the settlement and load sharing of the piled rafts in soft ground supporting the three buildings having different average stress were investigated based on the static and dynamic monitoring results.

3. ACCELERATION RESPONSE

The seismic responses of the 12-story and 7-story buildings during the 2011 Tohoku Earthquake (on March 11, M= 9.0, about 380 km distance from the epicentre) were successfully recorded through the seismic monitoring system. No evidence of soil liquefaction in the ground around the 12-story and 7-story buildings was found.

Figure 3 shows the acceleration time histories recorded near the ground surface, on the raft and the 1st floor of the 12-story building in the EW direction. The peak acceleration on the 1st floor was significantly reduced by the action of the base-isolation system. The peak ground acceleration was 1.75 m/s^2. Figure 4 shows the acceleration time history recorded on the first floor of the 7-story building in the EW direction. The peak acceleration was 1.21 m/s^2 and slightly greater than that on the raft in the 12-story building. Figure 5 shows the Fourier spectra of the EW accelerations of the ground at the site of the 12-story building. It can be seen that components of the periods of around 1 s were predominant.

Figure 6 shows the acceleration time history at the K-NET Urayasu strong motion station, near the 4-story building. No liquefaction occurred at K-NET Urayasu, while extensive soil liquefaction occurred in the reclaimed land of Urayasu City where the 4-story building is located (Tokimatsu et al., 2012). The peak acceleration was 1.57 m/s^2 in the EW direction.

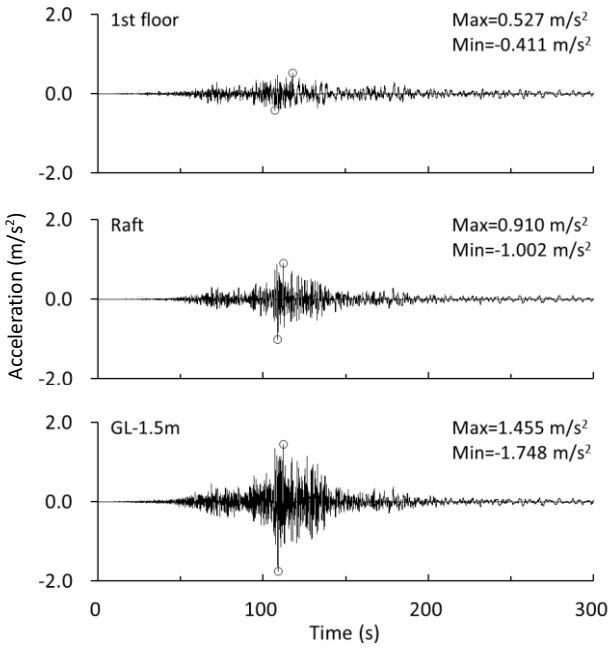

Figure 3 Acceleration time histories at the site of 12-story building (EW)

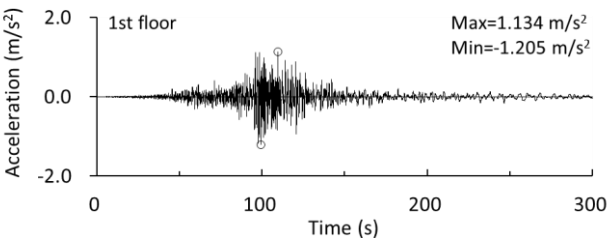

Figure 4 Acceleration time history on the1st floor of 7-story building (EW)

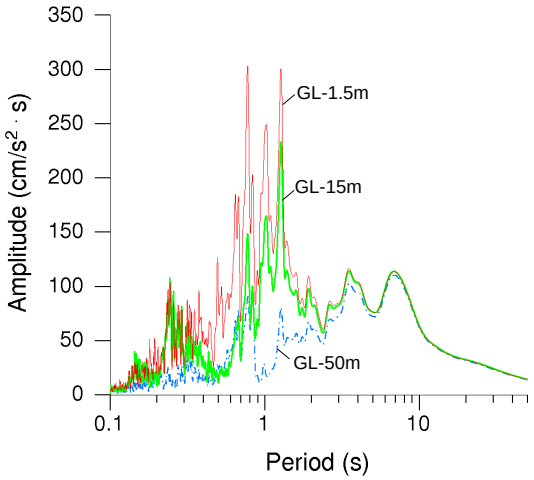

Figure 5 Fourier spectra of ground accelerations at the site of 12-story building (EW)

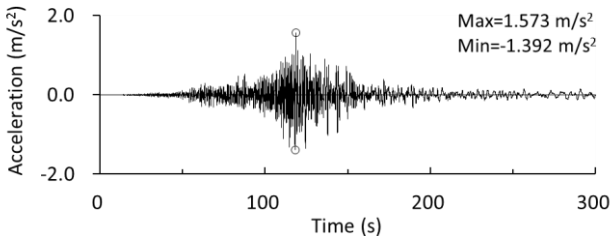

Figure 6 Acceleration time history (K-NET Urayasu, EW)

4. OVERVIEW OF STATIC MONITORING

To corroborate the foundation design, field monitoring on the settlement and the load sharing between the piles and the raft was performed from the beginning of the construction to over ten years after E.O.C.

4.1 Twelve-story building

Figure 7 shows the measured vertical ground displacements near the center of the raft. Since the vertical ground displacement just below the raft (at a depth of 5.8 m) after the casting of the raft might have been approximately equal to raft settlement, the vertical settlement refers as raft settlement. The raft settlement reached 17.3 mm on March 10, 2011, just before the 2011 Tohoku Earthquake. After the earthquake, the raft settlement increased by 0.3 mm from the pre-earthquake value to 17.6 mm on March 15, 2011. Thus, no significant change in raft settlement was observed after the earthquake. Thereafter, the raft settlements ranged from 16.7 to 17.8 mm and were found to be quite stable.

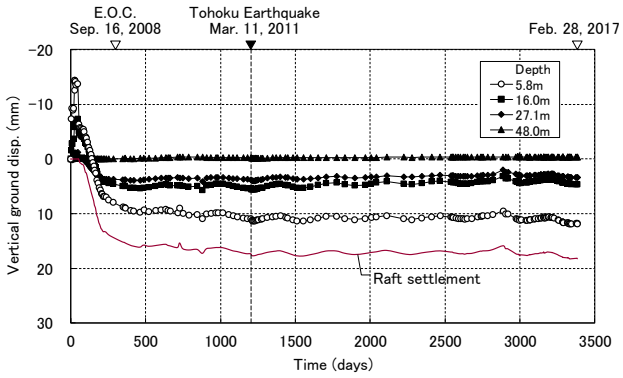

Figure 7 Measured vertical ground displacements below raft

Figure 8 shows the development of the measured axial loads of piles 5B and 7B. The axial load near the pile head (at 6.0-m depth) of Pile 7B decreased very slightly just after the earthquake, while that of Pile 5B changed little. Figure 9 shows the development of the measured contact stress between the raft and the soil and that between the raft and the deep mixing walls (DMW), together with the pore-water pressure beneath the raft. The contact stress between the raft and the DMWs near the periphery (D2) increased slightly after E.O.C., while the contact stress in the inner part (D1) was almost constant.

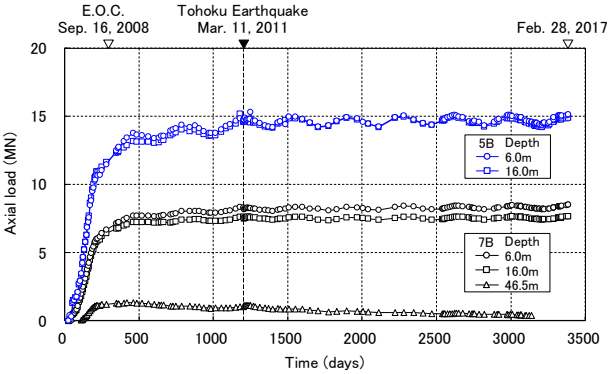

Figure 8 Measured axial loads of Piles 5B and 7B

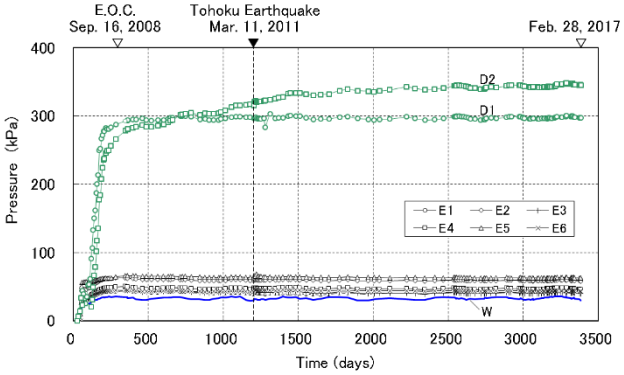

Figure 9 Measured contact pressure and pore-water pressure

Figure 10 shows the time-dependent load sharing among the piles, the DMW, the soil and the buoyancy in the tributary area of columns 5B and 7B. The sum of the measured pile-head loads and the raft load in the tributary area after E.O.C. was 35.4-39.8 MN. Here, the raft load means the sum of the total load carried by the DMW and that by the soil. The sum of the measured pile-head loads and the raft load in the tributary area is of 36.0 MN, which is roughly the same as the sum of the design load for columns 5B and 7B.

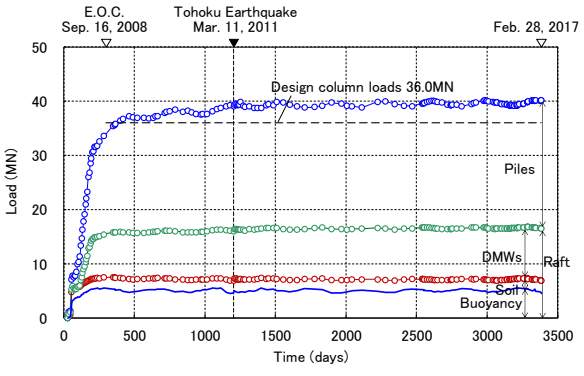

Figure 10 Load sharing among piles, DMWs and soil

Figure 11 shows the load sharing among the piles, the DMW and the soil in the tributary area of the columns 5B and 7B versus time. The ratio of the vertical load carried by the piles to the net load was estimated to be 0.67 just before the earthquake. The net load means the gross load minus the buoyancy. At that time, the ratio of the effective load carried by the DMW was estimated to be 0.26, while the ratio of the effective load carried by the soil was 0.07. It is seen that no significant change in load sharing among the piles, the DMW and the soil were observed after the earthquake. Thereafter, the load sharing was quite stable.

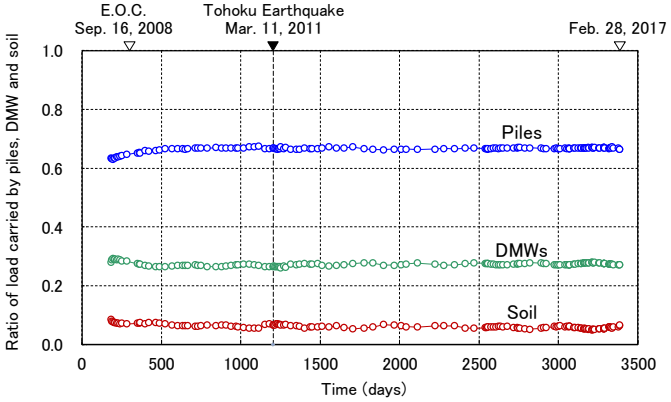

Figure 11 Load sharing of net load among piles, DMWs and soil

4.2 Seven-story building

Figure 12 shows the development of the measured vertical ground displacement under the raft. The raft settlement (vertical ground displacement at a depth of 3.0 m) reached 22.3 mm on March 10, 2011, just before the 2011 Tohoku earthquake. On March 15, 2011, the raft settlement increased by 1.1 mm to 23.4 mm. The increase in raft settlement was mostly due to vertical ground displacement between depths of 3.0 and 11.6 m. Thereafter, the raft settlement was found to be stable. Figure 13 shows the measured incremental settlements on the first floor between December 13, 2008 and May 29, 2011. The measured settlements after the earthquake were 14-33 mm. The incremental settlements were approximately equal to those induced by the earthquake, and the maximum increment was 6 mm while no change in maximum angular rotation was observed after the event.

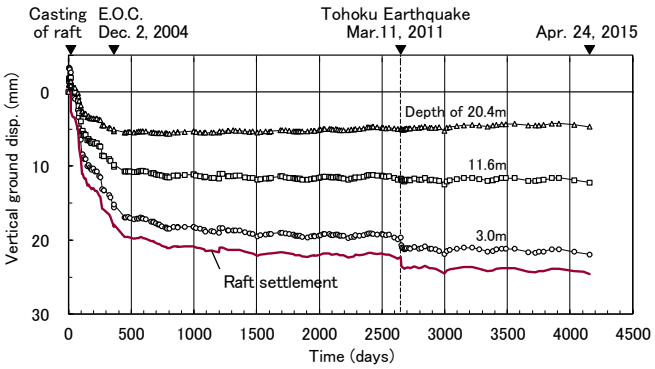

Figure 12 Measured vertical ground displacements below raft

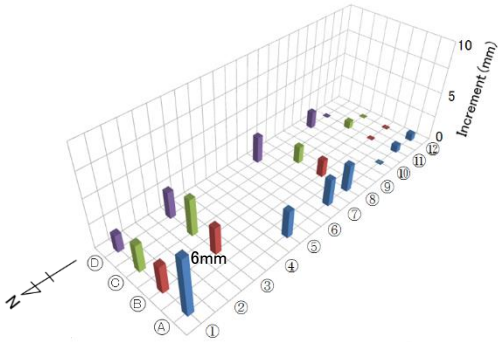

Figure 13 Incremental settlement at 1st floor after earthquake

Figure 14 shows the development of the measured axial forces of Piles 7A and 7B (where a positive sign means compression). The axial force near the pile head (at a depth of 4.3 m) reached 5.18 MN on Pile 7A and 5.62 MN on Pile 7B on March 10, 2011. On March 15, 2011, the pile head load of Pile 7A increased by 0.42 MN to 5.60 MN while that of Pile 7B increased by 0.26 MN to 5.88 MN. Figure 15 shows the development of the measured contact stress between the raft and the soil beneath the raft (where a positive sign means compression). After the earthquake, no significant changes in contact stress from both of E1 and E2 were observed.

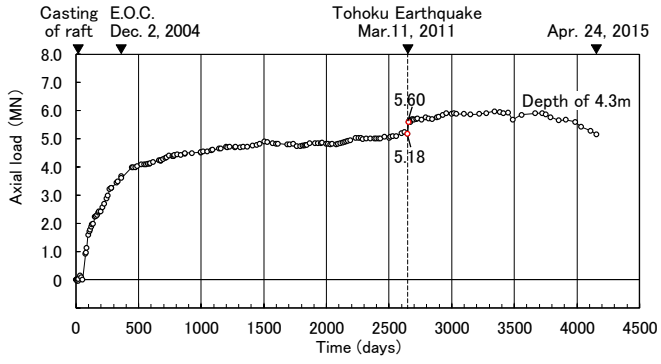

(a) Pile 7A

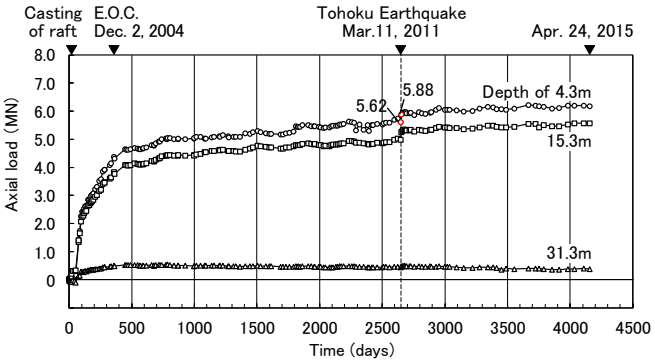

(b) Pile 7B

Figure 14 Measured axial loads of Piles 7A and 7B

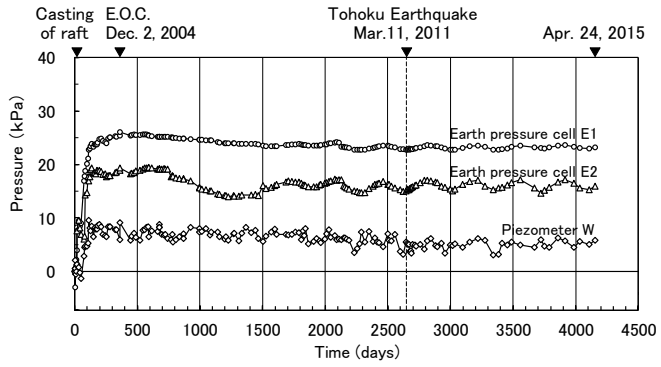

Figure 15 Measured contact pressure and pore-water pressure

Figure 16 shows the development of the sum of the loads carried by the piles and the soil in the tributary area of the columns 7A and 7B. The sum of the loads showed an abrupt increase at the time of the 2011 earthquake. This suggests that the contact stress between the raft and the DMWs decreased considerably after the earthquake. Assuming that the gross structure load is identical to the design load, the ratio of the load carried by the piles to the net load was estimated to be 0.72 just before the earthquake and increased to 0.76 on March 15, 2011. Subsequently, the ratio of the load carried by the piles to the net load increased to 0.81 at maximum about three years after the event.

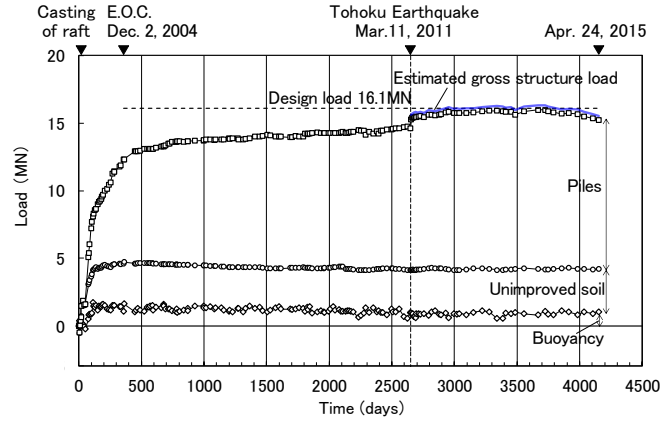

Figure 16 Load sharing between piles and soil

4.3 Four-story building

Figure 17 shows the development of the measured vertical ground displacements just below the mat slab. The vertical displacement near 3C (in the north part of the building) was 16 mm before the earthquake (November 2010) and increased by 7 mm to 23 mm after the earthquake, in May 2011. Thereafter, the settlement was almost stable. On the other hand, the vertical displacement near 17C (in the south part of the building) increased gradually after E.O.C. due to the continuing consolidation settlement. The settlement was 41 mm before the earthquake and increased to 63 mm in May 2014. In contrast to the settlement near 3C, Figure 17 suggests that no substantial increase in settlement near 17C was induced by the earthquake.

Figure 18 shows the development of the vertical ground displacement of each soil layer near 17C. In May 2014, seven and a half years after E.O.C., the largest displacement of 43 mm occurred in the clayey layer between depths of 42.0 and 60.0 m. The consolidation settlement was likely to be caused by the structure load via the piles in addition to the residual land subsidence. In contrast, the displacements of the sand and clayey layers between the depths of 3.6 and 42.0 m were relatively small. This indicates that the consolidation settlement of the clayey layer have almost completed. It should be noted that a small amount of consolidation settlement in the clayey layer between the depths of 15 and 22.2 m began to occur after the event, possibly due to dissipation of the earthquake-induced pore-water pressure.

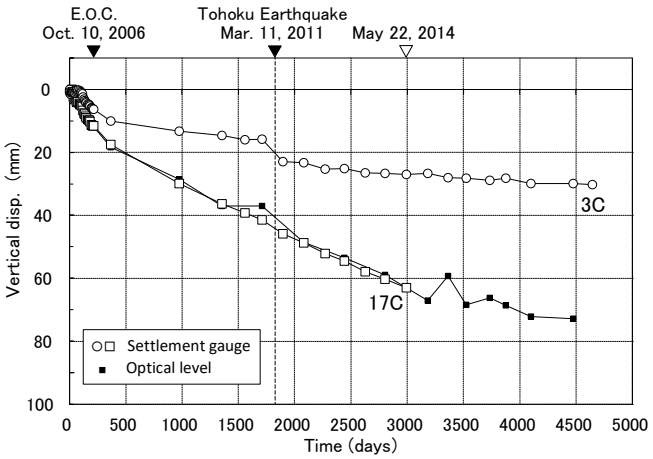

Figure 17 Measured vertical ground displacements just below mat slab

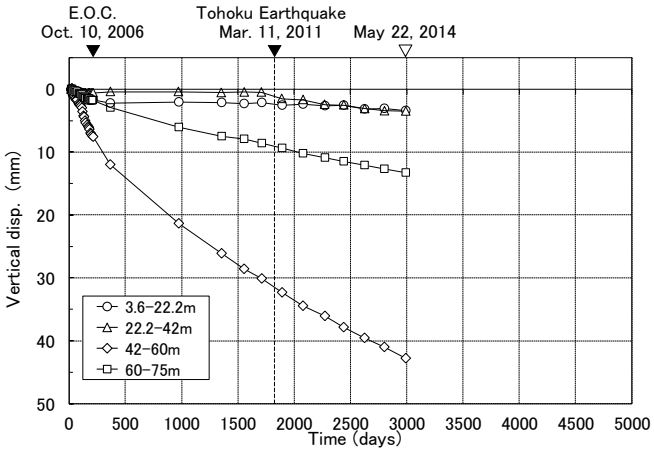

Figure 18 Measured vertical ground displacements of each soil layer (near 17C)

Figure 19 shows the measured settlement profiles of the first-floor. At the end of the observation, the maximum settlement and angular rotation in the north-south direction along Street E were 105 mm and 1/1690, respectively. There appeared no significant change in the settlement profile before and after the earthquake.

Figure 20 shows the measured axial load near the pile head of Piles 3C and 17C (at depths of 3.9 and 3.5 m, respectively). The axial load of Pile 3C four months before the earthquake, decreased considerably two months after the earthquake. The ratio of the load carried by the pile to the design load in the tributary area of the column 3C (7.8 MN) reduced from 0.50 to 0.27. In contrast, the axial load of Pile 17C before the earthquake showed almost no change after the earthquake. The ratio of the load carried by the piles (assumed to be twice the measured load of Pile 17C) to the design load in the tributary area of the column 17C (8.0 MN) decreased only slightly from 0.70 to 0.67. Subsequently, the ratio of the load carried by the Piles 3C and 17C to the design load increased gradually to 0.34 and 0.77, respectively, at the end of the observation.

Figure 21 shows the measured contact stress and pore-water pressure beneath the mat slab near 3C and 17C. No significant change in the contact stress was observed after the earthquake. This indicates that the effectiveness of the grid-form DMWs as a countermeasure of soil liquefaction against seismic motion with PGA of 2.0 m/s^2 was confirmed (Uchida et al, 2012).

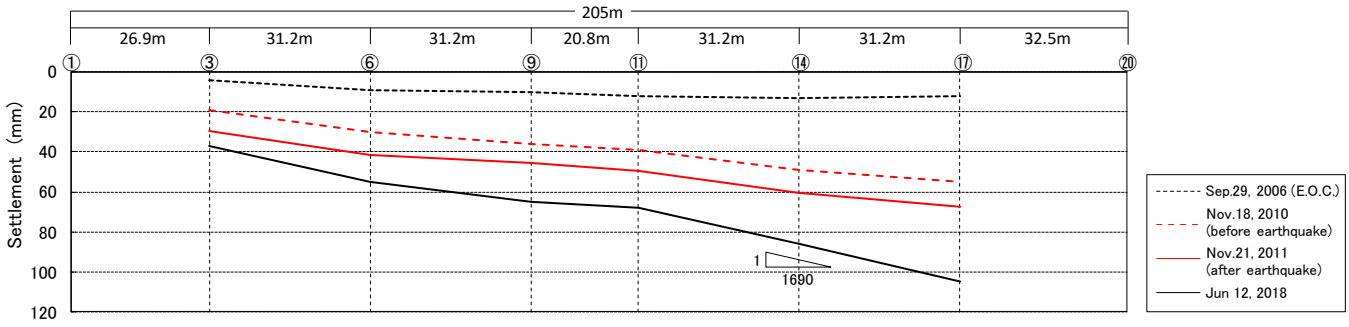

Figure 19 Settlement profiles at 1st floor (Street C)

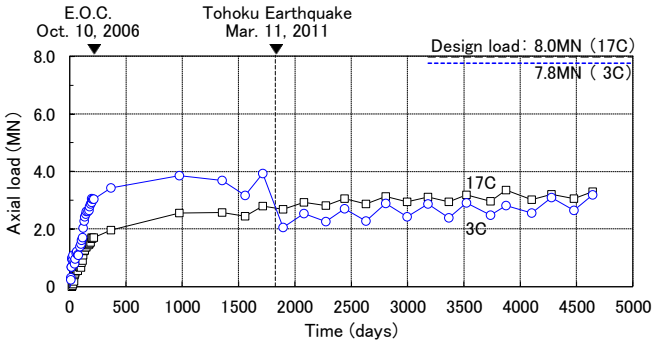

Figure 20 Measured axial loads at pile head

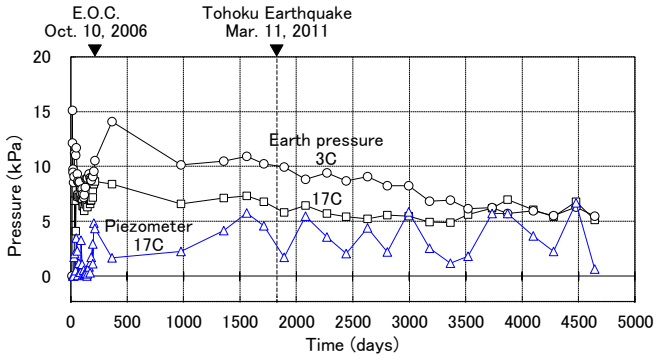

Figure 21 Measured contact pressure and pore-water pressure

5. DISCUSSION

5.1 Load transfer along piles

The time histories of the incremental axial forces in Piles 5B and 7B of the 12-story building and those in Pile 7B are shown in Figure 22. In Figure 22(b), the axial forces were obtained as the sum of the incremental force shown in Figure 22(a) and the pre-earthquake axial load (in the static monitoring on March 10, 2011). The axial force near the pile head of Pile 7B decreased slightly from the pre-earthquake value near the end of the event (600 s after the start of the event), while that of Pile 5B showed almost no change. The ratio of the maximum amplitude to the pre-earthquake value near the pile head for Pile 7B was 8.4% in compression and 12.4% in tension, while that for Pile 5B was 5.8% in both compression and tension. It appeared that the incremental forces on the piles in the mid-rise building was relatively small due to the action of the base isolation system.

The time histories of the incremental axial forces in Pile 7B of the 7-story building are shown in Figure 23. In Figure 23(b), the axial force near the pile head of Pile 7B increased slightly near the end of the event. The ratio of the maximum amplitude to the pre-earthquake value near the pile head was 8.5%.

Figure 24 shows the incremental axial force at the pile head versus the incremental shaft resistance, and that versus the incremental force at the pile toe (where a positive sign means upward resistance). As for Pile 7B of the 12-story building (toe-bearing pile), the lower frictional force (16.0-46.5 m) and the pile toe force tend to increase with the increase in pile head force. In contrast, the upper frictional force (6.0-16.0 m) was very small and had no correlation with the increase in pile head force, as is also seen in Figure 22(a). As for Pile 7B of the 7-story building (the shaft-bearing pile), the similar tendency is seen in relations of the incremental pile head force with the frictional force and pile toe force.

It is worthwhile note that the ratio of the incremental pile-toe force to the incremental pile-head force for the end-bearing pile was roughly 0.5 during 0-130 s and increased to1.0 during 130-300 s, while the ratio of the incremental lower shaft frictional force to the incremental pile-head force was 0.6 during 0-130 s and decreased significantly during 130-300 s. Thus, it was found that the toe resistance of the toe-bearing pile was mobilized significantly under the repeated vertical loading, even though the pile length was very long (45 m). As for the shaft-bearing pile, the ratio of the incremental pile-toe force to the incremental pile-head force (around 0.3) was considerably less than the ratio of the lower frictional force to the pile head force, but markedly greater than that of the pile-toe force to the pile-head force in the static measurement just before the event (an order of 0.1).

The time histories of the incremental contact stress in the 12-story and 7-story buildings are shown in Figures 25 and 26, respectively. The contact stress between the raft and the soil in the 7-story building was very small compared to those in the 12-story building.

5.2 Settlement

The vertical ground displacement during the earthquake was recorded in the 7-story building. Figure 27 shows the time history of the incremental vertical displacement between the depths of 3.0 and 11.6 m including principal motions, together with that of incremental pile-head axial force of Pile 7B. There appears to be a strong in-phase correlation between the increments in ground displacement and pile head load. Figure 28 shows the relationship between the incremental pile-head axial force and the incremental vertical ground displacement. It is seen that inelastic displacement occurred due to penetration of the pile subjected to repeated loading resulted from the rocking moment of the superstructure, while the residual displacement was very small (Yamashita et al., 2016). Thereafter, the settlement increased from 0.7 to 1.0 mm on March 15, as shown in Figure 28. Figure 29 shows the pore-water pressure induced by the earthquake in the silty soil underneath the raft. The pore-water pressure near the end of the event was small and similar in the two buildings, around 0.5 kPa. Therefore, a small amount of consolidation settlement might have occurred in the silty soil due to dissipation of the pore-water pressure shown in Figure 29(b).

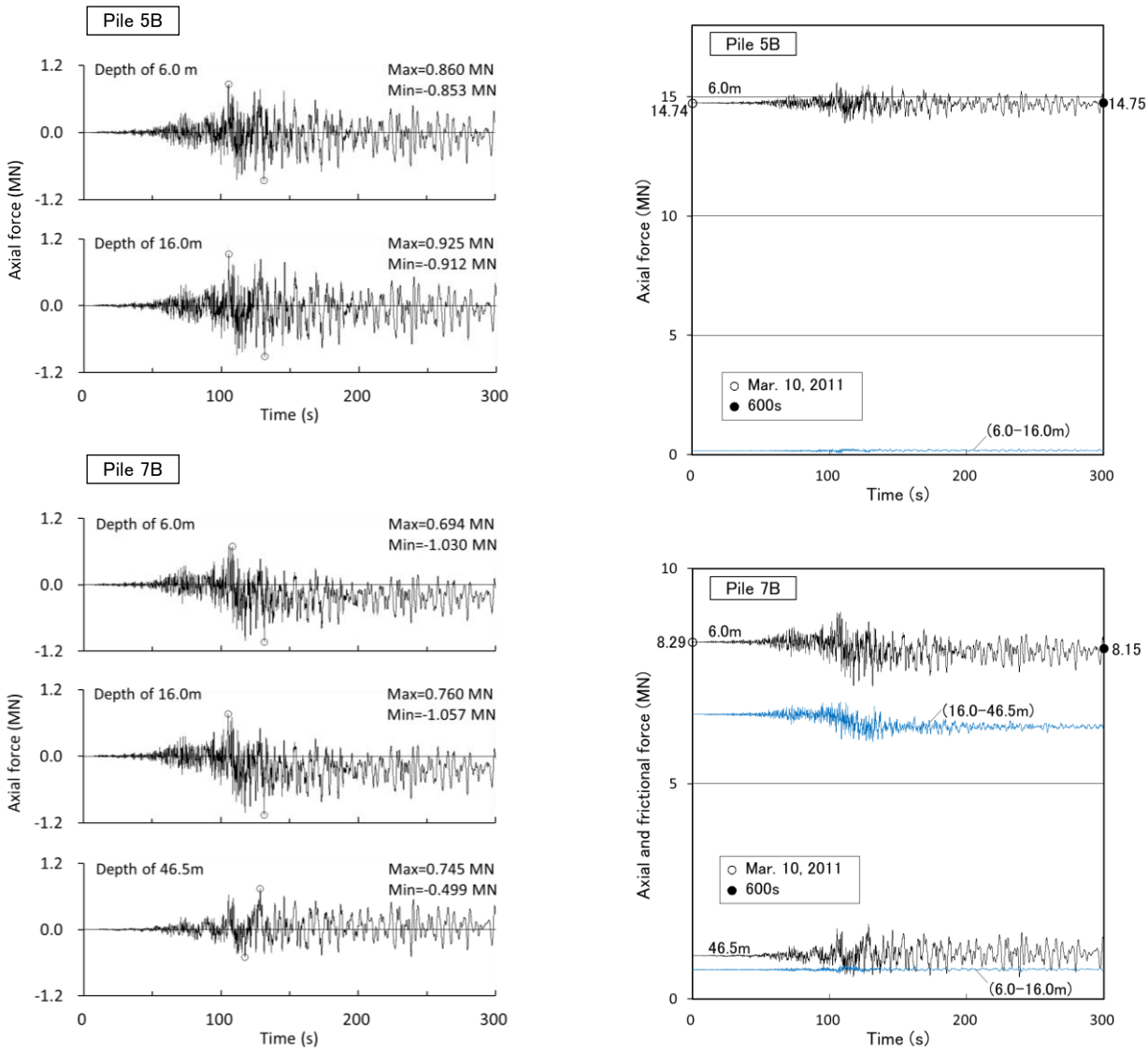

(a) Increments in axial forces (b) Axial and frictional forces

Figure 22 Time histories of increments in axial forces of piles (12-story building)

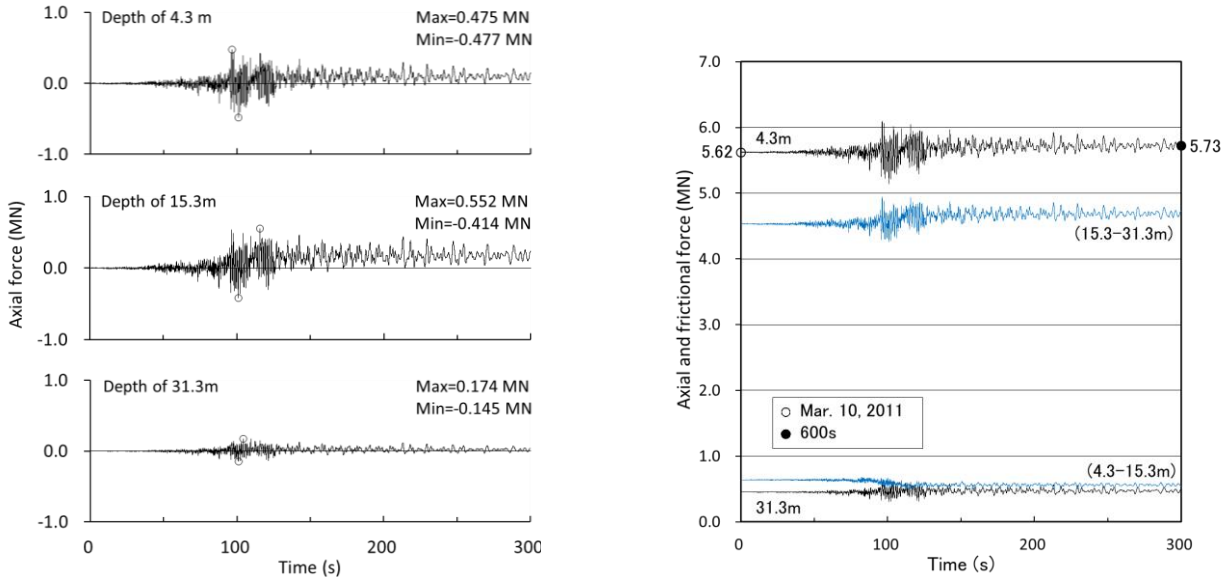

(a) Time histories of incremental axial forces (b) Axial and frictional forces

Figure 23 Time histories of increments in axial forces of Pile 7B (7-story building)

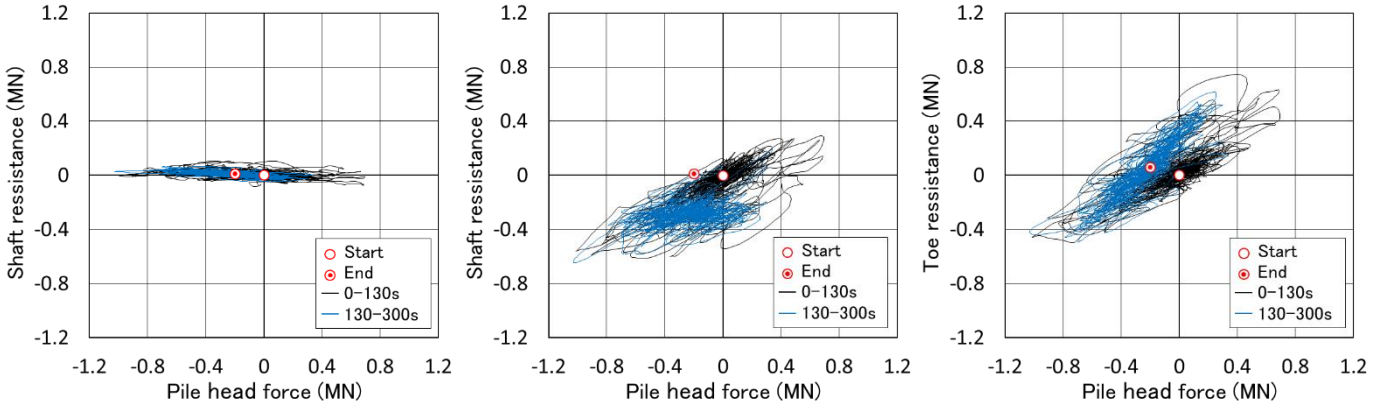

Pile head force vs. shaft resistance (6.0-16.0 m) Pile head force vs. shaft resistance (16.0-46.5 m) Pile head force vs. toe resistance (46.5 m)

(a) Pile 7B (12-story building)

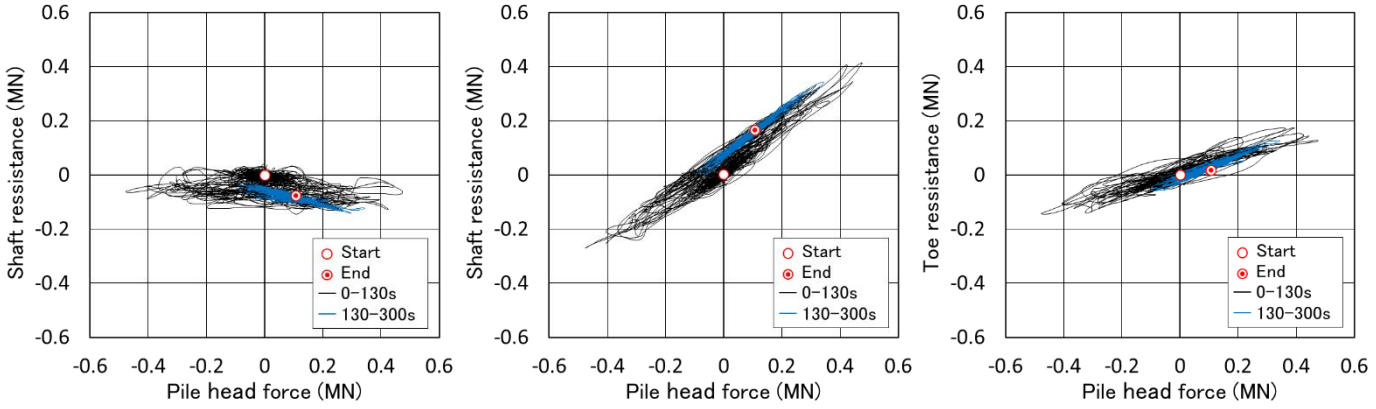

Pile head force vs. shaft resistance (4.3-15.3 m) Pile head force vs. shaft resistance (15.3-31.3 m) Pile head force vs. toe resistance (31.3 m)

(b) Pile 7B (7-story building)

Figure 24 Incremental pile head axial force vs. incremental shaft resistance, and that vs. incremental toe resistance

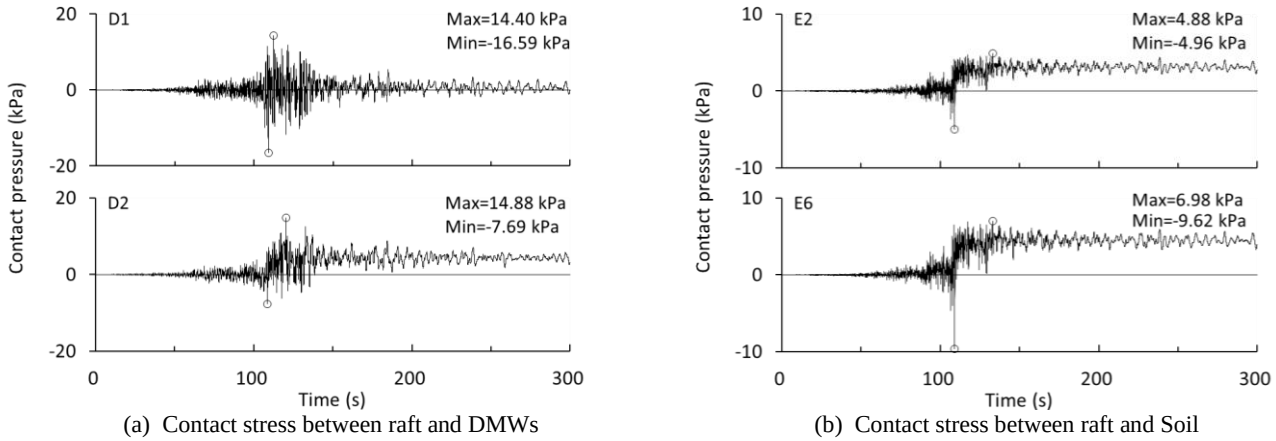

(a) Contact stress between raft and DMWs (b) Contact stress between raft and Soil

Figure 25 Increments in contact pressures (12-story building)

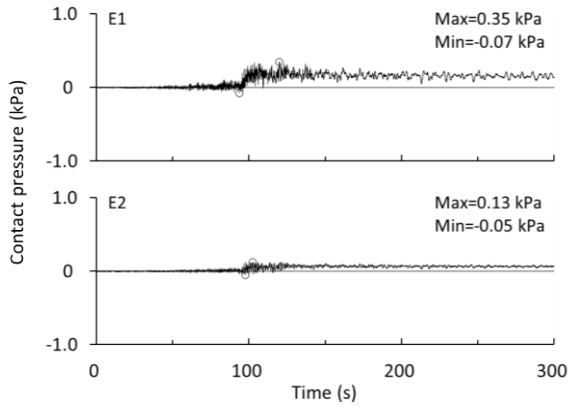

Figure 26 Increments in contact stress (7-story building)

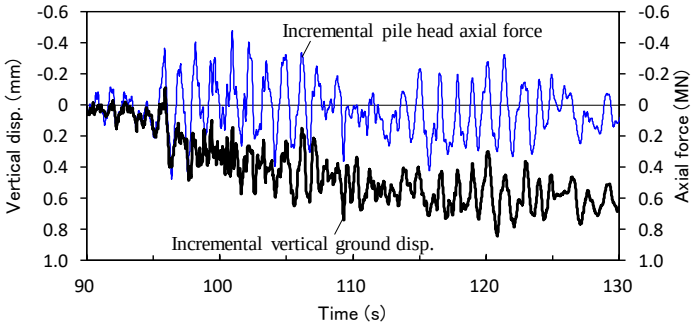

Figure 27 Time history of incremental vertical ground displacement (3.0-11.6 m), and that of incremental pile-head axial force of Pile 7B

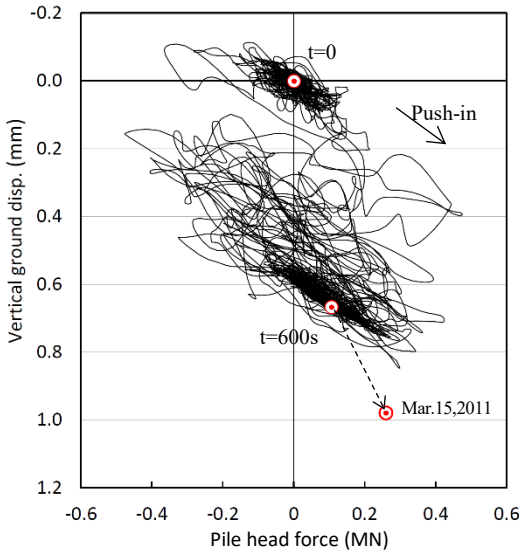

Figure 28 Incremental pile head axial force of Pile 7B vs. incremental vertical ground displacement (3.0-11.6m)

As for the three buildings, small residual settlements of the raft (1-7 mm) were observed after the earthquake in the cases using relatively short shaft-bearing piles, i.e., 7-story building and 4-story building (northern part), while little change in settlement was observed for the toe-bearing piles or long shaft-bearing piles, i.e., 12-story building and 4-story building (southern part).

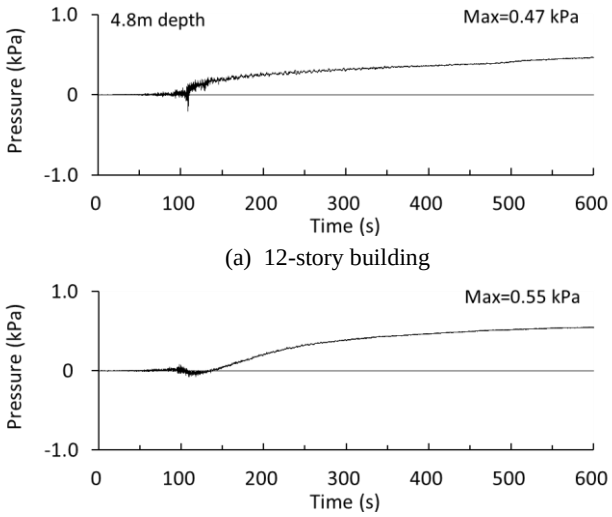

(a) 12-story building

(b) 7-story building

Figure 29 Excess pore-water pressure underneath raft

5.3 Load sharing between piles and raft

Figure 30 shows the ratios of the load carried by the piles to the net load in the tributary area after E.O.C. versus time. For the 4-story building, "the ratio to the net load" means the design load minus the buoyancy as calculated using the measured pore-water pressure (17C).

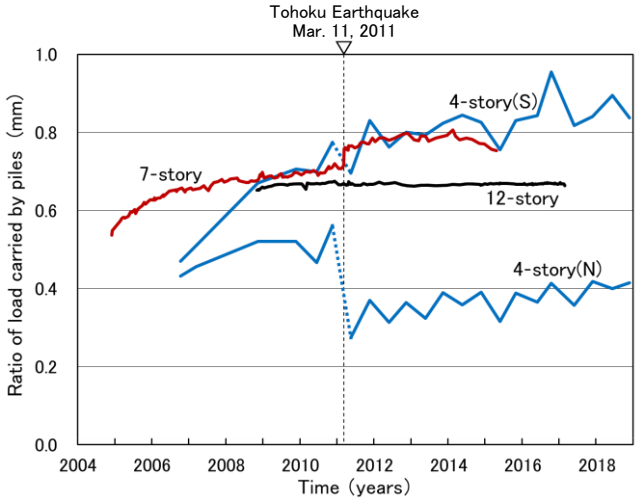

Figure 30 Ratios of load carried by piles to net load vs. time

An obvious change in the ratio of the pile load was observed after the earthquake in the cases using relatively short shaft-bearing piles. In the 7-story building, the load carried by the piles increased slightly during the earthquake as shown in Figure 23(b), in addition, the contact stress between the raft and the soil increased very slightly as is seen in Figure 26. This means that some amount of load transfer from the DMWs to the piles occurred; possibly due to a small amount of immediate settlement of the DMWs (whose bottom was in the very soft silty soil). The increment in axial load carried by the piles from the pre-earthquake value was 0.12 MN near the end of the event. It increased slightly thereafter to 0.26 MN on March 15, as shown in Figure 28, possibly due to the consolidation settlement caused by the dissipation of the pore-water pressure shown in Figure 29(b). In the 4-story building (northern part), a considerable decrease in axial load of Pile 3C combined with load transfer from the piles to the DMWs

occurred after the event; possibly due to the settlement of shaft-bearing piles (Yamashita et al., 2019). After the earthquake, the load carried by the piles increased due to the consolidation settlement of the clayey layers as is seen in Figure 17.

On the other hand, no significant change in the ratio of the pile load was observed for the toe-bearing piles or long shaft-bearing piles after the earthquake. The load sharing between the piles and the raft generally depends on relative stiffness of the raft and the piles. When the stiffness of the piles as well as that of the raft are virtually elastic under seismic loading, no significant change in the load sharing occurs. The monitoring results suggest that the maximum axial force acting on the piles during the earthquake was significantly less than the bearing capacity of the piles. In the 12-story building, the load carried by Pile 7B decreased during the earthquake as shown in Figure 22(b) while the load carried by both the soil (E6) and the DMWs (D2) increased as is seen in Figure 25. Hence, a very small amount of load transfer from the piles to both the soil and the DMWs occurred near the periphery of the raft. After the earthquake (on March 15, 2011), the ratio of the load carried by the piles increased to almost the same value as the pre-earthquake value due to dissipation of the pore-water pressure shown in Figure 29(a) (Yamashita et al., 2012).

Consequently, it was found that some amount of change in load sharing between the piles and the raft was caused by the small settlements of the raft in such the cases using relatively short shaft-bearing piles, while no significant change in the ratio was observed in the cases using toe-bearing piles or long shaft-bearing piles.

6. CONCLUSIONS

Through the investigation of the effects of seismic action on the settlement and load sharing behaviour of the piled rafts in soft ground supporting three buildings, the following conclusions can be drawn:

(1) During the earthquake, the toe resistance of the pile embedded in very dense sandy stratum was mobilized significantly under the vertical loading, even though the pile length was very long. On the other hand, the toe resistance of the shaft-bearing pile in the clayey soil was considerably less than the lower shaft frictional resistance, however, the ratio of the incremental pile-toe force to the incremental pile-head force was markedly greater than that of the pile-toe force to the pile-head force obtained from the static measurement just before the earthquake.

(2) Small residual settlements of the raft (1-7 mm) were observed after the earthquake in the cases using relatively short shaft-bearing piles, i.e., 7-story building and 4-story building (northern part), while little change in raft settlement was observed for the toe-bearing piles or long shaft-bearing piles, i.e., 12-story building and 4-story building (southern part). Thus, it was found that no significant change in foundation settlement was observed after the earthquake.

(3) Some amount of change in load sharing between the piles and the raft might have been caused by the small settlements of the raft in the cases using relatively short shaft-bearing piles, while almost no change in the load sharing was observed in the cases using toe-bearing piles or long shaft-bearing piles.

7. ACKNOWLEDGEMENTS

The authors are grateful to Dr. A. Uchiba of Takenaka Corporation for his contribution to seismic design of the piled raft system.

8. REFERENCES

Hamada, J., Aso, N., Hanai, A., and Yamashita, K. (2015) “Seismic performance of piled raft subjected to unsymmetrical earth pressure based on seismic observation records”, Proc. of the 6th Int. Conf. on Earthquake Geotechnical Engineering.

Katzenbach, R., Arslan, U., and Moormann, C.（2000) “Piled raft foundation projects in Germany”, Design applications of raft foundations, Hemsley J.A. Editor, Thomas Telford, pp323-392.

Mandolini, A., Russo, G., and Viggiani, C. (2005) “Pile foundations: Experimental investigations, analysis and design”, Proc. of the 16th ICSMGE, Vol. 1, pp177-213.

Mendoza, M.J., Romo, M.P., Orozco, M., and Dominguez, L. (2000) “Static and seismic behavior of a friction pile-box foundation in Mexico City clay”, Soils & Foundations, 40(4), pp143-154.

National Research Institute for Earth Science and Disaster Prevention (NIED). K-NET, <http://www.k-net.bosai.go.jp/>.

Poulos, H.G. (2001) “Piled raft foundations: design and applications”, Geotechnique(2), pp95-113.

Poulos, H. G. (2016) “Lessons learned from designing high-rise building foundations”, Geotechnical Engineering Journal of the SEAGS & AGSSEA, 47(4), pp35-49.

Tokimatsu, K., Tamura, S., Suzuki, H., and Katsumata, K. (2012) “Building damage associated with geotechnical problems in the 2011 Tohoku Pacific Earthquake”, Soils & Foundations, Vol52(5), pp956-974.

Uchida, A., Yamashita, K., and Odajima, N. (2012) “Performance of piled raft foundation with grid-form ground improvement during the 2011 off the Pacific Coast of Tohoku Earthquake”, Journal of Disaster Research, 7(6), pp. 726-732.

Yamashita, K., Yamada, T., and Hamada, J. (2011a) “Investigation of settlement and load sharing on piled rafts by monitoring full-scale structures”, Soils & Foundations, 51(3), pp513-532.

Yamashita, K., Hamada, J., and Yamada, T. (2011b) “Field measurements on piled rafts with grid-form deep mixing walls on soft ground”, Geotechnical Engineering Journal of the SEAGS & AGSSEA, 42(2), pp1-10.

Yamashita, K., Hamada, J., Onimaru, S., and Higashino, M. (2012) “Seismic behavior of piled raft with ground improvement supporting a base-isolated building on soft ground in Tokyo”, Soils & Foundations, 52(5), pp1000-1015.

Yamashita, K., Hamada, J., and Tanikawa, T. (2016) “Static and seismic performance of a friction piled combined with grid-form deep mixing walls in soft ground”, Soils & Foundations, 56(3), pp559-573.

Yamashita, K., Hamada, J., and Tanikawa, T. (2017) “Seismic behavior of piled raft in soft ground based on field monitoring”, Proc. of International Symposium on Design and Analysis of Piled Raft Foundations, pp215-234.

Yamashita, K., Tanikawa, T., and Uchida, A. (2019) “Long-term behaviour of piled raft with DMW grid on reclaimed land”, Geotechnical Engineering Journal of the SEAGS & AGSSEA, 50(3) (to be published).